

Protein crystallization in hydrogel beads

Ronnie Willaert,* Ingrid Zegers,
Lode Wyns and Mike Sleutel

Department of Ultrastructure, Flanders
Interuniversity Institute for Biotechnology, Vrije
Universiteit Brussel, B-1050 Brussels, Belgium

Correspondence e-mail:
ronnie.willaert@vub.ac.be

Received 2 June 2005

Accepted 6 July 2005

The use of hydrogel beads for the crystallization of proteins is explored in this contribution. The dynamic behaviour of the internal precipitant, protein concentration and relative supersaturation in a gel bead upon submerging the bead in a precipitant solution is characterized theoretically using a transient diffusion model. Agarose and calcium alginate beads have been used for the crystallization of a low-molecular-weight (14.4 kDa, hen egg-white lysozyme) and a high-molecular-weight (636.0 kDa, alcohol oxidase) protein. Entrapment of the protein in the agarose-gel matrix was accomplished using two methods. In the first method, a protein solution is mixed with the agarose sol solution. Gel beads are produced by immersing drops of the protein–agarose sol mixture in a cold paraffin solution. In the second method (which was used to produce calcium alginate and agarose beads), empty gel beads are first produced and subsequently filled with protein by diffusion from a bulk solution into the bead. This latter method has the advantage that a supplementary purification step is introduced (for protein aggregates and large impurities) owing to the diffusion process in the gel matrix. Increasing the precipitant, gel concentration and protein loading resulted in a larger number of crystals of smaller size. Consequently, agarose as well as alginate gels act as nucleation promoters. The supersaturation in a gel bead can be dynamically controlled by changing the precipitant and/or the protein concentration in the bulk solution. Manipulation of the supersaturation allowed the nucleation rate to be varied and led to the production of large crystals which were homogeneously distributed in the gel bead.

1. Introduction

Mass transport in classical protein crystallization methods, *i.e.* hanging and sitting drops (vapour diffusion), batch crystallization, dialysis and liquid–liquid diffusion, is influenced by buoyant convective flows. Gravity causes either crystal sedimentation or density-driven and convective flows generated around growing crystal surfaces (Carotenuto *et al.*, 2002). Microgravity experiments have shown that crystallization in a diffusive environment can result in high-quality crystals (McPherson, 1993; DeLucas, 2001; García-Ruiz, Drenth *et al.*, 2001; Vergara *et al.*, 2003; Snell & Helliwell, 2005). The extent of quality improvement has been reported for numerous examples. For example, microgravity-grown crystals of pike parvalbumin diffracted beyond 0.9 Å compared with 1.7 Å for earth-grown crystals (Declercq *et al.*, 1999), the diffraction resolution of canavalin crystals was improved from 2.6 to 1.7 Å (Ko *et al.*, 2001) and a dramatic increase in crystal volume and an increase in diffraction resolution was found for

Table 1

Examples of protein crystal growth in gels.

Protein	Gel type	Gel concentration [% (w/v)]	Crystallization system	Reference
Alliinase	Agarose	0.5	GCB†	Garcia-Ruiz <i>et al.</i> (2002)
Anti-lysozyme camel antibody	Agarose	0.5	GCB†	Garcia-Ruiz <i>et al.</i> (2002)
Apoferitin	Agarose	0.3	Pasteur pipette	Chernov <i>et al.</i> (2001)
AP-Sm1 protein	Agarose	0.1–0.2	Glass capillary	Biertümpfel <i>et al.</i> (2002)
Aspartyl tRNA synthetase-1	Agarose	0.1–0.2	Limbrot plates	Lorber, Sauter, Ng <i>et al.</i> (1999)
Bacteriophage T4 endonuclease VII	Agarose	0.08–0.3	Glass capillary	Zhu <i>et al.</i> (2001)
Canavalin	Agarose	0.1–0.2	Sitting-drop gel	Biertümpfel <i>et al.</i> (2002)
Catalase	Agarose	0.2–0.6	Microdialysis gel	Thiessen (1994)
Concanavalin A	Agarose	0.5	GCB†	Garcia-Ruiz <i>et al.</i> (2002)
Cytochrome <i>c</i>	Agarose	0.5	GCB†	Garcia-Ruiz <i>et al.</i> (2002)
Dehydroquinase (type II)	Agarose	0.5	GCB†	Garcia-Ruiz <i>et al.</i> (2002); Maes <i>et al.</i> (2004)
Factor XIII	Agarose	0.5	GCB†	Garcia-Ruiz <i>et al.</i> (2002)
Ferritin	Agarose	0.5	Glass tube	Gavira & Garcia-Ruiz (2002)
Glucose isomerase	Agarose	0.5	GCB†	Garcia-Ruiz <i>et al.</i> (2002)
Hfq protein	Agarose	0.5	GCB†	Garcia-Ruiz <i>et al.</i> (2002)
Hf _q protein	Agarose	0.1–0.2	Glass capillary	Biertümpfel <i>et al.</i> (2002)
FBPase	Agarose	0.5	GCB†	Garcia-Ruiz <i>et al.</i> (2002)
Insulin	Agarose	0.5	GCB†	Garcia-Ruiz <i>et al.</i> (2002)
Lysozyme	Silica (TMS)‡	2–5% (v/v)	Glass tube	Robert & Lefauchaux (1988)
	Silica (TMS)‡	1.4% (v/v)	Glass capillary	Vidal <i>et al.</i> (1999)
	Agarose	0.2–0.6	Sitting-drop gel	Thiessen (1994)
	Agarose	0.5	Microdialysis gel	
	Agarose	0.5	GCB†	Garcia-Ruiz <i>et al.</i> (2002)
	Agarose	0.2	Glass tube	Dong <i>et al.</i> (1999)
	Agarose	1	Glass capillary	Vidal <i>et al.</i> (1999)
	Agarose	0.15–0.3	Lindemann glass capillary	Lorber, Sauter, Ng <i>et al.</i> (1999)
	Agarose	0.5	Glass tube	Gavira & Garcia-Ruiz (2002)
	Gellan gum	0.25	Interferometric cell	Hou <i>et al.</i> (2001)
Lumazine synthase	Agarose	0.5	GCB†	Garcia-Ruiz <i>et al.</i> (2002)
(Pro-Pro-Gly) ₁₀	Agarose	0.5	GCB†	Garcia-Ruiz <i>et al.</i> (2002)
Thaumatococin	Agarose	0.5	Glass tube	Gavira & Garcia-Ruiz (2002)
	Agarose	0.15–0.3	Lindemann glass capillaries	Lorber, Sauter, Ng <i>et al.</i> (1999)
	Agarose	0.15	APCF§ dialysis reactor	Lorber, Sauter, Robert <i>et al.</i> (1999); Sauter <i>et al.</i> (2002)
Tomato Bushy Stunt Virus	Agarose	0.5	GCB†	Garcia-Ruiz <i>et al.</i> (2002)
Triose phosphate isomerase	Agarose	0.1–0.2	Lindemann glass capillary	Lorber, Sauter, Ng <i>et al.</i> (1999)
Trypsin	Agarose	0.5	GCB†	Garcia-Ruiz <i>et al.</i> (2002)
Xylanase	Agarose	0.4	Glass tube	Robert & Lefauchaux (1988)
	Agarose	0.5	GCB†	Garcia-Ruiz <i>et al.</i> (2002)

† Granada Crystallization Facility. ‡ Tetramethoxysilane. § Advanced Protein Crystallization Facility.

manganese superoxide dismutase crystals (Vahedi-Faridi *et al.*, 2003). Other protein crystals that have shown increased diffraction resolution upon growth in microgravity include alcohol dehydrogenase (Esposito *et al.*, 2002), human antithrombin III (Skinner *et al.*, 1997; Wardell *et al.*, 1997), apoc-rustacyanin C₁ (Habash *et al.*, 2003), catalase (Ko *et al.*, 1999), human Bence–Jones protein (Alvarado *et al.*, 2001), human serum albumin (He & Carter, 1992), insulin (Smith *et al.*, 2003), mistletoe lectin (Krauspenharr *et al.*, 2002), myoglobin (Miele *et al.*, 2003), NAD synthetase (Symersky *et al.*, 2002), photosystem I (Klukas *et al.*, 1999), [(Pro-Pro-Gly)₁₀]₃ (Berisio *et al.*, 2002) and serine protease (Betzel *et al.*, 2001). In some cases, no or only a small improvement in resolution has also been observed (*e.g.* Strong *et al.*, 1992).

It has been suggested that small-molecule impurities and macromolecular aggregates might be responsible for crystal defect formation, which decreases crystal quality and size (Vekilov *et al.*, 1995; Vekilov & Rosenberger, 1996; McPherson

et al., 1996; Chernov, 1997). The improvement in crystal quality has been attributed to a lower incorporation of impurities during diffusion-limited growth of tetragonal hen egg-white lysozyme (Carter *et al.*, 1999). Theoretical analysis showed that in this case the stagnant solution around a growing crystal was strongly depleted with respect to impurities.

In the absence of stirring or other fast fluid motion, the incorporation of protein molecules into the growing crystal produces a concentration-depletion zone around the crystal. The size and shape of this depletion zone are controlled by the coupled transport of the crystallizing molecules *via* diffusion in solution to the growing surface and the crystal-growth kinetics. Mach–Zehnder interferometry has been used to observe the depletion zone and intrinsic kinetics (*e.g.* Hou *et al.*, 2001; Otálora *et al.*, 2002). The impurity-depletion zone surrounding apoferritin crystals growing in gel with a holo-ferritin dimer impurity could be observed visually (Chernov *et*

al., 2001). Colourless holoferritin crystals grown in the presence of iron-containing red-coloured ferritin dimers were surrounded by colourless zones depleted with respect to this dimer.

Diffusion-limited growth of protein crystals can easily be obtained on earth by using hydrogel crystallization (Henisch, 1988; Robert & Lefaucheur, 1988; Robert *et al.*, 1999; García-Ruiz, Novella *et al.*, 2001). An agarose concentration as low as 0.04% (*w/v*) was able to overcome buoyancy and crystal sedimentation (García-Ruiz, Novella *et al.*, 2001). Agarose, agar, silica and gellan gum have been successfully used as gel materials to obtain protein crystals (Table 1). Agarose has been particularly frequently employed. The spectrum of potential available hydrogels which could be used for protein crystallization is much wider. Many types of hydrogels have been used for the immobilization of enzymes and living cells for very different applications (Willaert & Baron, 1996; Nedovic & Willaert, 2004, 2005). These gels can also be tested for protein crystallization.

Only limited research has been performed to investigate the influence of the gel on nucleation and crystal growth. It has been shown using small-angle neutron scattering (SANS) that protein (lysozyme) interactions are identical in agarose-gel and gel-free media (Vidal *et al.*, 1998a). However, lysozyme-cluster formation was increased in agarose gel. Since nuclei would be built out of these clusters, it was concluded that agarose gel is a nucleation promoter. The observed nucleation enhancement in agarose gels could also arise from an apparent supersaturation: agarose fibres trap water during the gelling process and therefore the protein concentration in gelled solutions is not identical to that in the blank experiments without agarose (Gavira & García-Ruiz, 2002). Characterization of lysozyme solution trapped in a silica-gel network (using SANS) shows an adsorption of protein on the gel surface through electrostatic and most probably through hydrogen-bonding interactions (Vidal *et al.*, 1998b). The consecutive decrease of concentration is consistent with the decrease of nucleation rate with respect to gel-free solutions. Consequently, silica gel could be classified as a nucleation inhibitor. Using small-angle X-ray scattering, it has been shown that a decrease in temperature and/or an increase in crystallizing agent induces an increase in the attractions present in lysozyme solutions, with the lysozyme remaining monomeric. Similar behaviour has been observed when agarose gels are used (Finet *et al.*, 1998).

Gel-grown crystals can lead to enhanced diffraction properties. Previously unachieved high-resolution X-ray diffraction data have been obtained for thaumatin crystals that were grown in 0.15% (*w/v*) agarose gel (Sauter *et al.*, 2002). These crystals have a lower mosaicity and yield data sets with 20% higher signal-to-noise ratio than controls obtained by conventional convective solution growth (Lorber, Sauter, Robert *et al.*, 1999). Crystallization in gellified media also prevents crystal sedimentation. This favours three-dimensional growth (García-Ruiz, Novella *et al.*, 2001; Lorber & Giegé, 2001). Gels also provide an efficient protection of samples during handling (mounting, soaking, seeding *etc.*) and

transport without affecting their crystallographic analysis (García-Ruiz *et al.*, 2002; Sauter *et al.*, 2002). Additionally, their presence can be crucial for preserving the diffraction properties during cryocooling. This has been demonstrated for aspartyl-tRNA synthetase crystals (Zhu *et al.*, 2001).

Various crystals have been grown in gel systems (see Table 1). Most systems have a cylindrical geometry. The use of capillaries in protein crystallization has been reviewed by García-Ruiz (2003). Glass capillaries have been used to perform liquid-liquid counter-diffusion protein crystallization in space. These systems have subsequently been used for ground experiments in a batch mode. An example is the Granada Crystallization Box (GCB), which has been commercialized by Hampton Research (García-Ruiz *et al.*, 2002). The GCB consists of a narrow polystyrene box (dimensions 102 × 35 × 5 mm) and a capillary holder which can hold six glass capillaries. Owing to the properties of the counter-diffusion experiment, each position in the capillary is subjected at different varying supersaturation conditions. Various protein crystals have already been grown in the GCB (Table 1).

In this contribution, we present the technique of performing protein crystallization in hydrogel beads. A theoretical diffusion model is used to calculate the precipitant and protein concentration and relative supersaturation evolution in a gel bead at pre-nucleation conditions and to characterize its behaviour. Owing to its fast response time, supersaturation profiles in a gel bead can be controlled well by changing the external conditions. The usefulness of this technique is illustrated for the crystallization of lysozyme in agarose and calcium alginate hydrogel beads and of alcohol oxidase in agarose beads.

2. Materials and methods

2.1. Mass-transport calculations

The diffusion of salt into a gel bead containing protein is described by its mass balance,

$$\frac{\partial C'_s}{\partial t} = \frac{D_{e,s}}{R^2} \left(\frac{\partial^2 C'_s}{\partial r'^2} + \frac{2}{r'} \frac{\partial C'_s}{\partial r'} \right), \quad (1)$$

where C'_s is the dimensionless salt concentration which equals $C_s/C_{s,b}$ (C_s is the salt concentration in the gel bead and $C_{s,b}$ is the salt concentration in the bulk), R the bead radius, r' ($= r/R$) the dimensionless radial distance, t the time and $D_{e,s}$ the salt effective diffusion coefficient in the gel. It is assumed that external mass-transport limitation can be neglected. In this case, the initial and boundary conditions can be written as

$$C'_s(0, r') = 0 \text{ for } r' < 1 \text{ and } C'_s(0, 1) = 1, \quad (2)$$

$$C'_s(t, 1) = 1 \text{ and } \left(\frac{\partial C'_s}{\partial r'} \right)_{r'=0} = 0. \quad (3)$$

Likewise, the diffusion of protein in the gel bead towards the surrounding medium can be expressed as

$$\frac{\partial C'_p}{\partial t} = \frac{D_{e,p}}{R^2} \left(\frac{\partial^2 C'_p}{\partial r'^2} + \frac{2}{r'} \frac{\partial C'_p}{\partial r'} \right), \quad (4)$$

where C'_p is the dimensionless protein concentration, which equals $C_p/C_{p,i}$ (C_p is the protein concentration in the gel bead and $C_{p,i}$ is the initial concentration), and $D_{e,p}$ is the protein effective diffusion coefficient in the gel. The initial and boundary conditions are

$$C'_p(0, r') = C_{p,i} \text{ for } r' < 1 \text{ and } C'_p(0, 1) = 0, \quad (5)$$

$$C'_p(t, 1) = 0 \text{ and } \left(\frac{\partial C'_p}{\partial r'} \right)_{r'=0} = 0. \quad (6)$$

The supersaturation is computed as the relative supersaturation (Otálora & García-Ruiz, 1997),

$$\sigma = \frac{C_p}{C_{p,s}}, \quad (7)$$

where $C_{p,s}$ is the protein solubility concentration. The solubility curve of lysozyme for sodium chloride can be expressed as the sum of two Green-type functions (Otálora & García-Ruiz, 1997),

$$C_{p,s} = S_1 + S_2, \quad (8)$$

$$\ln(S_1) = \ln(0.97617) - 0.30376C_s \quad (9)$$

$$S_2 = 65.69255 \exp(-1.71840C_s), \quad (10)$$

where $C_{p,s}$ and C_s have dimensions of %(*w/v*). (10) was fitted to solubility data at low NaCl concentrations [this equation is different to the originally proposed equation of Otálora & García-Ruiz (1997), since this equation gives also an extrapolation for NaCl concentrations going to zero].

The partial differential equations (1) and (4) with the corresponding initial and boundary conditions were integrated by orthogonal collocation in the spatial coordinate (Villadsen & Michelsen, 1978). The resulting system of ordinary differ-

ential equations was next integrated by a fourth-order Runge-Kutta-Gill method.

2.2. Experimental methods

2.2.1. Gel-bead preparation: agarose beads. Commercial hen egg-white lysozyme (Lot 093K1455, Sigma) was dissolved in sodium acetate buffer pH 4.5 at room temperature. Agarose ('low gelling temperature', Gibco BRL) was dissolved in sodium acetate buffer pH 4.5 at boiling temperature. The lysozyme and agarose solutions were mixed at 310 K. Beads were formed upon dripping into a cold (277 K) paraffin solution. The beads had an average diameter of 3.5 mm. Gel beads containing 0.5 and 1%(*w/v*) agarose were produced. These beads contained a lysozyme concentration of 60 and 40 mg ml⁻¹, respectively.

Alcohol oxidase (AOX; Lot 081K1770, Sigma) from *Pichia pastoris* was diluted to the required concentration in 0.1 M Bis-Tris. 'Empty' agarose beads were filled by submerging them in the AOX solution (20 or 45 mg ml⁻¹, 0.1 M Bis-Tris) for 1 d at 277 K.

2.2.2. Gel-bead preparation: calcium alginate beads. Calcium alginate beads were produced by dripping a sodium alginate (Fluka) solution into a well stirred 0.27 M CaCl₂ solution. Gel beads containing 0.5, 1 and 1.5%(*w/v*) alginate were produced. The beads were cured during 1.5 h in the CaCl₂ solution and next washed in sodium acetate buffer (0.05 M, pH 4.5). The beads had an average diameter of 2.5 mm. Beads were filled with lysozyme by submerging them in a lysozyme solution (60 mg ml⁻¹, 0.05 M sodium acetate buffer pH 4.5) for 4 h.

2.2.3. Protein crystallization. All crystallization experiments were performed in a multi-well plate at 293 K. Lysozyme was crystallized at pH 4.5 (0.05 M sodium acetate) and alcohol oxidase at pH 7.0 (0.1 M Bis-Tris). In most experiments, one well contained one gel bead and the precipitation solution (1 ml or 100 μl in the case where the bulk concen-

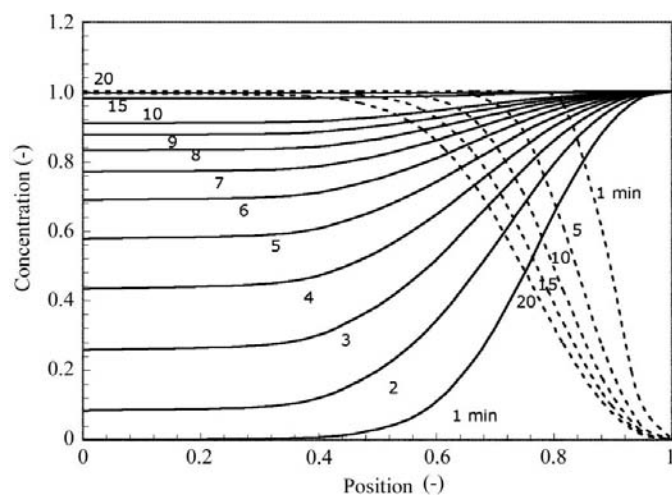


Figure 1 Evolution of the NaCl (unbroken lines) and lysozyme (broken lines) concentration in a 1%(*w/v*) agarose-gel bead during the first 20 min (the gel-bead edge is at position 1); bead diameter = 3.5 mm; $C_{p,i}$ = 40 mg ml⁻¹, $C_{s,b}$ = 7%(*w/v*) NaCl.

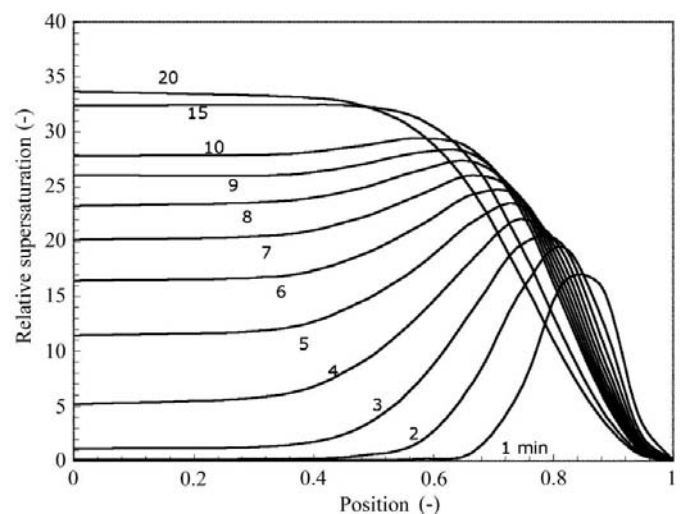


Figure 2 Evolution of the relative supersaturation in a 1%(*w/v*) agarose gel bead during the first 20 min (the gel-bead edge is at position 1); bead diameter = 3.5 mm; $C_{p,i}$ = 40 mg ml⁻¹, $C_{s,b}$ = 7%(*w/v*) NaCl.

tration also contains protein). NaCl was used as the precipitating agent for lysozyme crystallization and polyethylene glycol (PEG) 6000 for alcohol oxidase crystallization.

3. Results and discussion

3.1. Growth of lysozyme crystals in agarose beads

3.1.1. Evolution of the NaCl and lysozyme concentration and supersaturation profiles in agarose beads. The evolution of NaCl and lysozyme concentration in a gel bead which initially contained a uniformly distributed lysozyme concentration upon immersion into the precipitant solution was calculated (Fig. 1). The values of the parameters used were $D_{e,s} = 1.6 \times 10^{-9} \text{ m}^2 \text{ s}^{-1}$, $D_{e,p} = 0.9 \times 10^{-10} \text{ m}^2 \text{ s}^{-1}$, $C_{p,i} = 60 \text{ mg ml}^{-1}$, $C_{s,b} = 0.8 \text{ M}$ and a bead diameter of 3.5 mm. A quantitative measure to characterize how fast the concentration in the gel bead changes upon applying a step change in concentration at the edge of the bead is the response time (τ). As can be seen in Fig. 1, the response time of the diffusion of NaCl in the bead is much higher than the outward diffusion of lysozyme. The response time for diffusion of a molecule into or out a bead can be calculated as (Glueckauf, 1955)

$$\tau = \frac{R^2}{15D_e} \quad (11)$$

Using (11), the response time for NaCl is 2.1 min and for lysozyme 37.8 min (the bead volume is 22.5 μl). Since gel beads can be produced routinely with diameters ranging from 200 μm to a few millimetres, the response time can be considerably reduced. For example, a gel bead with a diameter

of 0.5 mm (0.07 μl) gives a response time of 2.6 s for NaCl and 46 s for lysozyme. By increasing the gel concentration, the effective diffusion coefficient will decrease and as a result τ will increase.

The calculated evolution of the relative supersaturation in the gel bead is shown in Fig. 2. Initially, a concentration peak is formed at the edge of the bead. This peak broadens and travels to the centre of the bead. Owing to the diffusion of protein out of the gel bead, the supersaturation in the gel layer close to the bead edge is too low to reach the critical value for nucleation and no crystals will be produced in this part of the bead.

3.1.2. Bead preparation and crystal-growth observation. Agarose-gel beads containing lysozyme were prepared by mixing a non-gelled agarose solution with an equal volume of lysozyme solution at 310 K and then dropping this solution in a cold (277 K) paraffin solution to initiate the gelling process. Gel beads were hardened at 277 K for 1 h and washed with the buffer that was used in the crystallization experiments in order to remove the paraffin solution. Next, lysozyme-containing agarose beads were submerged in the precipitant solution (NaCl).

The growth of lysozyme crystals in agarose-gel beads has been studied for varying NaCl bulk concentrations [1 ml 4, 5, 6, 7 and 8% (w/v) NaCl], agarose concentrations [0.5 and 1.0% (w/v)] and initial lysozyme concentrations in the gel beads (60 and 20 mg ml⁻¹) (Fig. 3). As predicted by the simulation of the supersaturation profiles, there was no nucleation and growth of crystals in the outer layer of the gel beads. The density of crystals is the highest at the bead centre. The number of crystals increases with the NaCl, agarose and lysozyme concentration. The fact that the increase in agarose concentration [0.5–1% (w/v)] resulted in a higher number of crystals confirms the results of Vidal *et al.* (1998a), who indicated that agarose gel is a nucleation promoter. Our results are in disagreement with those of Thiessen (1994), which indicated that agarose is only a nucleation promoter up to a concentration of 0.4% agarose. Other gel types can act as a nucleation inhibitor, such as silica gel (Vidal *et al.*, 1998b).

3.1.3. Influence of the supersaturation on the long-term crystal growth in gel beads. Agarose-gel beads [0.5% (w/v)] containing 60 mg ml⁻¹ lysozyme were submerged in 100 μl of 4.5, 5.0 and 5.5% (w/v) NaCl solution. Crystal growth was observed after 1 d and after one month (Fig. 4). There were no lysozyme crystals present in gel beads submerged in 4.5% (w/v) NaCl after 1 d. After one month, large crystals that were homogeneously distributed in the bead could be observed.

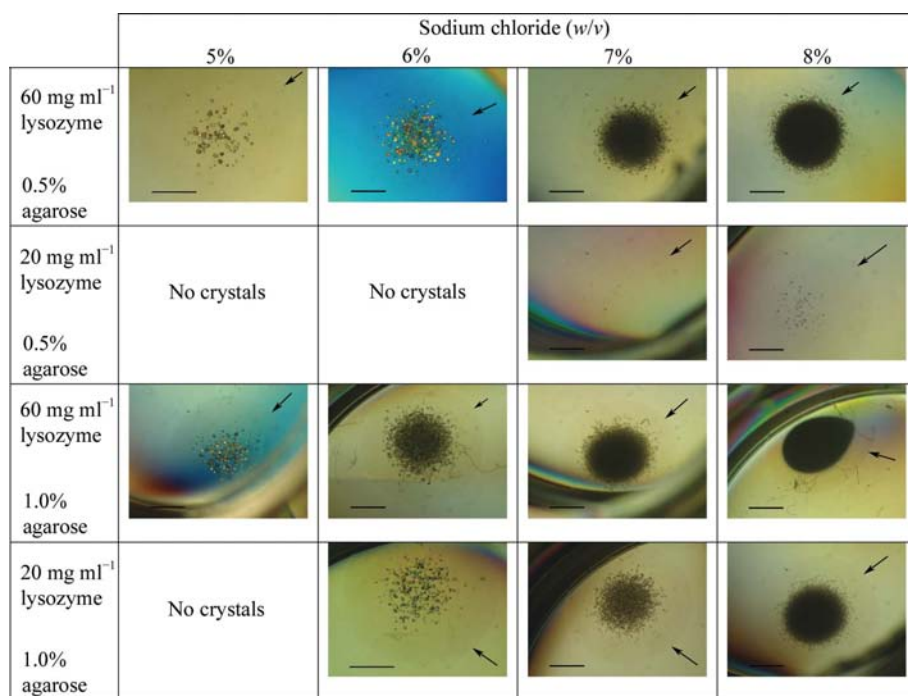


Figure 3 Crystallization of lysozyme in agarose-gel beads: influence of the NaCl concentration, agarose and lysozyme content. The arrow indicates the edge of the gel bead; the scale-bar length is 1 mm.

Crystals grown in 5.0 and 5.5% (w/v) NaCl were small after 1 d and their number was proportional to the increasing NaCl concentration. Large crystals were observed after one month of further growth. This experiment demonstrates that large lysozyme crystals can be grown in agarose-gel beads at a slow growth rate when the supersaturation is low.

3.1.4. Nucleation and growth control in a gel bead. Owing to the large surface area of a spherical crystallization system, the supersaturation in a gel bead can be changed during the nucleation and crystal-growth process by influencing the diffusion of precipitant and protein into and out of the bead. To prove this concept, the following experiment was performed. Three agarose-gel beads [0.5% (w/v); initially containing 60 mg ml⁻¹ lysozyme] were submerged in a precipitant solution containing a high [7% (w/v)] NaCl concentration to initiate crystal nucleation (and growth). As a reference bead, the first bead was kept submerged during the whole duration of the experiment in this solution. It can be observed (Fig. 5a) that a large number of small crystals are present in the centre of the bead (comparable to the experiment discussed in §3.1.2). The second bead was taken out of the initial well 15 min after the start of the experiment and placed in another well which contained a small volume (50 µl) of a precipitant solution containing 2% (w/v) NaCl and 40 mg ml⁻¹ lysozyme. It can be observed (Fig. 5b) that the number of crystals is considerably reduced and that they have a much larger size. The third bead was placed after 30 min in another well containing 2% (w/v) NaCl and 40 mg ml⁻¹ lysozyme solution. In this case, the centre of the bead contained a large number of small crystals (Fig. 5c), but at the edge of the bead rather large crystals were observed (in contrast to the reference bead). This experiment shows that the number of nuclei in a gel bead can be controlled by dynamically changing the supersaturation from a high value to a lower value. This can simply be accomplished by changing the precipitant concen-

tration surrounding the gel bead. This experiment also shows that the protein concentration in the gel bead can be controlled by changing the protein concentration gradient, which drives the diffusion process in the gel bead. This resulted in larger crystals in the second bead. In the third bead, the protein concentration in the outer layer (which was depleted in protein during the first part of the experiment) was increased owing to diffusion of lysozyme from the bulk solution into the gel bead. As a result, the supersaturation in the outer layer was increased and resulted in the nucleation and growth of relatively large lysozyme crystals.

3.2. Growth of lysozyme crystals in alginate-gel beads

Alginates, which are naturally occurring marine polysaccharides, have been used for several decades in the food and pharmaceutical industries as emulsifying, thickening, film-forming and gelling agents. Within the biomedical field, alginates are now also well known as immobilization materials for cells, tissue or macromolecules (Melvik & Dornish, 2004). The success of this method is mainly a consequence of the very mild conditions under which immobilization is performed and it is a fast, simple and cost-effective technique. The biocatalyst suspension is mixed with a sodium alginate solution and the mixture dripped into a solution containing multivalent cations (usually calcium). The droplets form gel spheres instantaneously, entrapping the biocatalyst in a three-dimensional lattice of ionically cross-linked alginate (ionotropic gel).

To our knowledge, protein crystallization in alginate hydrogels has not yet been discussed in the scientific literature. Therefore, we tested calcium alginate as a new protein crystallization environment. The classical method of mixing equal volumes of a protein solution with the sodium alginate solution before gelation takes place by dropping the mixture in a stirred CaCl₂ solution could not be used, since upon mixing the lysozyme solution with the sodium alginate solution a white precipitate formed. Therefore, another method was developed. Firstly, calcium alginate beads which do not contain lysozyme were produced. Next, the beads were submerged in a lysozyme solution, which allowed the diffusion of lysozyme into the beads. This method can also be applied if other gel-forming polymers are used for protein crystallization where the gellification process is performed under harsh conditions (such as gellification at a high temperature, extreme pH values or/and in the presence of organic solvents).

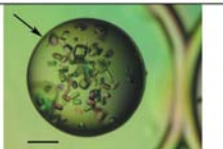
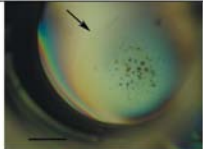
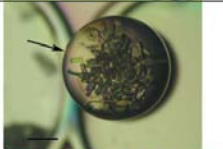
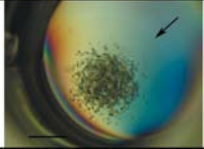
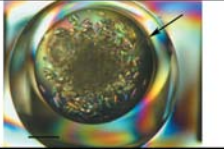
Sodium chloride (w/v)	Crystal growth observed after	
	1 day	1 month
4.5%	No crystals	
5.0%		
5.5%		

Figure 4
Influence of the supersaturation on the size of lysozyme crystals in agarose beads. The arrow indicates the edge of the gel bead; the scale-bar length is 1 mm.

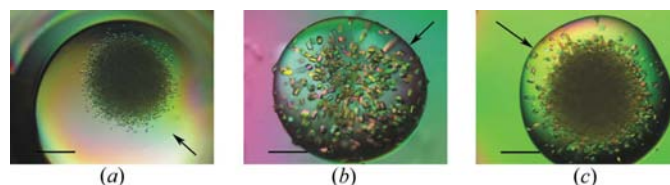


Figure 5
(a) Reference bead [crystallization in 7% (w/v) NaCl]; (b) gel bead kept for 15 min in 7% (w/v) NaCl and then in a 2% (w/v) NaCl solution containing 40 mg ml⁻¹ lysozyme; (c) gel bead kept for 30 min in 7% (w/v) NaCl and then in a 2% (w/v) NaCl solution containing 40 mg ml⁻¹ lysozyme. The arrow indicates the edge of the gel bead; the scale-bar length is 1 mm.

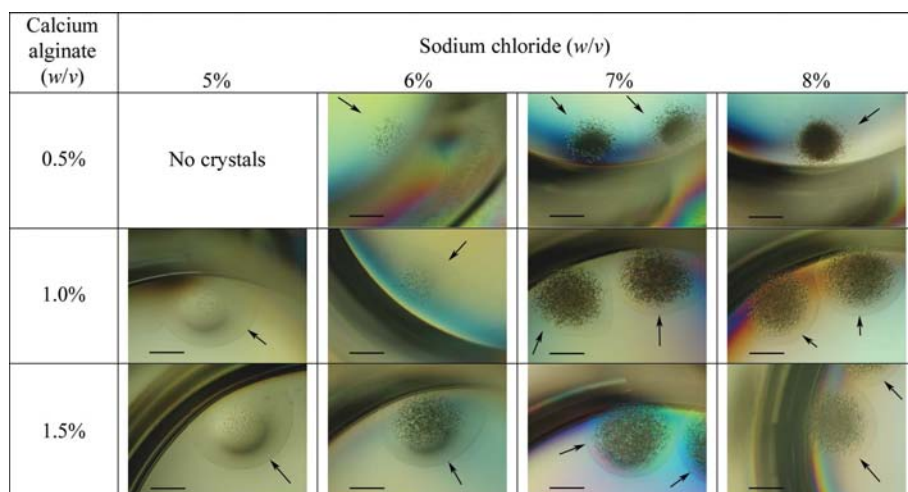


Figure 6
Crystallization of lysozyme in calcium alginate gel beads: influence of the NaCl and alginate concentration. The arrow indicates the edge of the gel bead; the scale bar length is 1 mm.

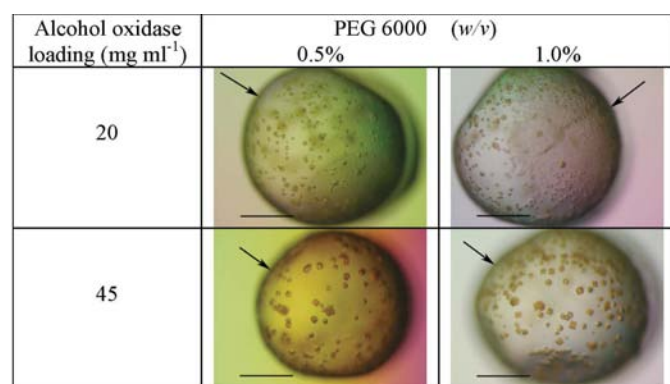


Figure 7
Crystallization of alcohol oxidase in agarose-gel beads: influence of the enzyme content and PEG 6000 concentration. The scale-bar length is 1 mm.

An additional advantage of this method is that the protein solution is purified upon diffusion into the gel bead (which can improve the quality of the crystals obtained in the beads).

The influence of the alginate concentration [0.5, 1.0 and 1.5% (w/v)] and NaCl concentration [4, 5, 6 and 7% (w/v)] was investigated. As in the case of lysozyme crystallization in agarose-gel beads, the number of crystals increases with increasing NaCl and gel concentration (Fig. 6). Consequently, calcium alginate gel is also a nucleation promotor.

A remarkable observation is that the morphology of the crystals that are embedded in the gel is changed: the crystals have a more globular, round shape. This was also observed for ferritin crystals grown in calcium alginate beads (unpublished results). The impact of this observation on the crystal quality will be investigated by X-ray diffraction in the near future.

3.3. Growth of alcohol oxidase crystals in agarose gel beads

Alcohol oxidase (AOX; EC 1.1.1.3) is one of the principal proteins involved in the metabolism of methanol. This enzyme has a molecular weight of about 600 kDa and consists of eight

identical subunits. To date, its molecular structure has not been solved owing to poor X-ray diffraction resolution: 6 Å (Tykarska *et al.*, 1990) and 2.7 Å (Boys *et al.*, 1989). This protein has been selected for use as a high-molecular-weight protein in crystallization experiments in agarose-gel beads.

The method of filling ‘empty’ gel beads by diffusional mass transport from a bulk solution into the bead has been applied. Therefore, empty agarose [0.5% (w/v)] gel beads were submerged into AOX solutions containing 20 and 45 mg ml⁻¹ protein, respectively. Crystallization experiments with 0.5 and 1% (w/v) PEG 6000 as precipitating agent were performed and crystals were observed after 1 d. The crystal size is

somewhat larger for the higher AOX concentration in the bead (Fig. 7). In contrast to lysozyme crystallization, AOX crystals are rather homogeneously distributed in the gel volume, which is explained by the large difference between response time for the precipitant (fast inward diffusion) and AOX (very slow outward diffusion). This experiment demonstrates that even proteins with a very large MW can diffuse into the beads and can be crystallized in the gel matrix.

4. Conclusions and perspectives

Microgravity experiments have shown that high-quality crystals can be obtained as a consequence of diffusional mass-transport conditions during crystal nucleation and growth. Similar protein crystallization conditions (only diffusional mass transfer) can be mimicked on earth by using hydrogels.

In this contribution, we explored the use of hydrogel beads as a new protein crystallization system. We showed that the protein crystallization environment can be controlled in this system, *i.e.* the nucleation rate and crystal growth can be influenced and optimized. The response time for spherical systems is proportional to the square of the radius. In the case of small beads, very small response times can be achieved. Gel beads can be used to control the supersaturation values at which nucleation and crystal growth take place. The supersaturation value can be controlled by changing either the precipitant concentration in the bulk of the solution or the concentration of the surrounding protein solution.

Gel beads have unique potential for use in the study of the effect of supersaturation on the three-dimensional growth rate and crystal quality in diffusion-controlled mass-transport conditions. For this application, a continuous crystallization reactor can be used. Initially, conditions for nucleation are applied. Next, the precipitant concentration is reduced until a specified supersaturation is reached (a supersaturation value outside the nucleation area in the phase diagram). To keep the protein concentration in the gel constant during crystal growth, protein can be added to the precipitant solution and

will diffuse into the bead. Since the manipulation of gel beads or their surrounding environment is very easy, they could be used in automated crystallization 'machines'.

Two methods have been used to entrap protein in agarose-gel beads. The first method is the classical immobilization method of entrapping biocatalysts in a gel, where the protein solution is mixed with a heated agarose solution before gellification takes place by dripping this mixture in a cold paraffin solution. In the second method, protein-free agarose beads are first produced and are next filled with protein by diffusional mass transport from the bulk solution into the bead. This method can be advantageous for protein samples that cannot withstand the (harsh) gelification conditions of certain hydrogel types and for samples that still contain large impurities (since an additional purification step is introduced by the diffusion through the gel matrix).

This work was supported by the European Space Agency (Prodex program), the Flanders Interuniversity Institute for Biotechnology (VIB) and the Research Council of the Vrije Universiteit Brussel.

References

- Alvarado, U. R., DeWitt, C. R., Shutz, B. B., Ramsland, P. A. & Edmundson, A. (2001). *J. Cryst. Growth*, **223**, 407–414.
- Berisio, R., Vitagliano, L., Mazzarella, L. & Zagari, A. (2002). *Protein Sci.* **11**, 262–270.
- Betzal, C., Gourinath, S., Kumar, P., Perbandt, M., Eschenburg, S. & Singh, T. P. (2001). *Biochemistry*, **40**, 3080–3088.
- Biertümpfel, C., Basquin, J., Suck, D. & Sauter, C. (2002). *Acta Cryst.* **D58**, 1657–1659.
- Boys, C. W. G., Hill, D. J., Stockley, P. G. & Woodward, J. R. (1989). *J. Mol. Biol.* **208**, 211–212.
- Carotenuto, L., Piccolo, C., Castagnolo, D., Lappa, M., Tortora, A. & García-Ruiz, J. M. (2002). *Acta Cryst.* **D58**, 1628–1632.
- Carter, D. C., Lim, K., Ho, J. X., Wright, B. S., Twigg, P. D., Miller, T. Y., Chapman, J., Keeling, K., Ruble, J., Vekilov, P. G., Thomas, B. R., Rosenberger, F. & Chernov, A. A. (1999). *J. Cryst. Growth*, **196**, 623–637.
- Chernov, A. A. (1997). *J. Cryst. Growth*, **174**, 354–361.
- Chernov, A. A., García-Ruiz, J. M. & Thomas, B. R. (2001). *J. Cryst. Growth*, **232**, 184–187.
- Declercq, J. P., Evrard, C., Carter, D., Wright, B., Etienne, G. & Parello, J. (1999). *J. Cryst. Growth*, **196**, 595–601.
- DeLucas, L. J. (2001). *Drug Discov. Today*, **6**, 734–744.
- Dong, J., Boggon, T. J., Chayen, N. E., Raftery, J., Bi, R.-C. & Helliwell, J. R. (1999). *Acta Cryst.* **D55**, 745–752.
- Esposito, L., Sica, F., Raia, C. A., Giordano, A., Rossi, C. K., Mazzarella, L. & Zagari, A. (2002). *J. Mol. Biol.* **318**, 463–477.
- Finet, S., Bonneté, F., Frouin, J., Provost, K. & Tardieu, A. (1998). *Eur. Biophys. J.* **27**, 263–271.
- García-Ruiz, J. M. (2003). *Methods Enzymol.* **368**, 130–154.
- García-Ruiz, J. M., Drenth, J., Riès-Kautt, M. & Tardieu, A. (2001). *A World Without Gravity – Research in Space for Health and Industrial Processes*, edited by B. Fitton & B. Batrick, pp. 159–171. Noordwijk, The Netherlands: ESA.
- García-Ruiz, J. M., Gonzalez-Ramirez, L. A., Gavira, J. A. & Otálora, F. (2002). *Acta Cryst.* **D58**, 1638–1642.
- García-Ruiz, J. M., Novella, M. L., Moreno, R. & Gavira, J. A. (2001). *J. Cryst. Growth*, **232**, 165–172.
- Gavira, J. A. & García-Ruiz, J. M. (2002). *Acta Cryst.* **D58**, 1653–1656.
- Glueckauf, E. (1955). *Trans. Faraday Soc.* **51**, 1540–1551.
- Habash, J., Boggon, T. J., Raftery, J., Chayen, N., Zagalsky, P. F. & Helliwell, J. R. (2003). *Acta Cryst.* **D59**, 1117–1123.
- He, X. M. & Carter, D. C. (1992). *Nature (London)*, **358**, 209–215.
- Henisch, H. K. (1988). *Crystals in Gels and Liesegang Rings*. Cambridge University Press.
- Hou, W. B., Kudryavtsev, A. B., Bray, T. L., DeLucas, L. J. & Wilson, W. W. (2001). *J. Cryst. Growth*, **232**, 265–272.
- Klukas, O., Schubert, W.-D., Jordan, P., Kraub, N., Fromme, P., Witt, H. T. & Saenger, W. (1999). *J. Biol. Chem.* **11**, 7351–7360.
- Ko, T.-P., Day, J., Malkin, A. J. & McPherson, A. (1999). *Acta Cryst.* **D55**, 1383–1394.
- Ko, T.-P., Kuznetsov, Y. G., Malkin, A. J., Day, J. & McPherson, A. (2001). *Acta Cryst.* **D57**, 829–839.
- Krauspenharr, R., Rypniewski, W., Kalkura, N., Moore, K., DeLucas, L., Stoeva, S., Mikhailov, A., Voelter, W. & Betzel, Ch. (2002). *Acta Cryst.* **D58**, 1704–1707.
- Lorber, B. & Giegé, R. (2001). *J. Cryst. Growth*, **231**, 252–261.
- Lorber, B., Sauter, C., Ng, J. D., Zhu, D. W., Giegé, R., Vidal, O., Robert, M. C. & Capelle, B. (1999). *J. Cryst. Growth*, **204**, 357–368.
- Lorber, B., Sauter, C., Robert, M.-C., Capelle, B. & Giegé, R. (1999). *Acta Cryst.* **D55**, 1491–1494.
- McPherson, A. (1993). *J. Phys. D*, **26**, B104–B112.
- McPherson, A., Malkin, A. J., Kuznetsov, Y. G. & Koszelak, S. (1996). *J. Cryst. Growth*, **168**, 74–92.
- Melvik, J. E. & Dornish, M. (2004). *Fundamentals of Cell Immobilization Biotechnology*, edited by V. Nedovic & R. Willaert, pp. 33–51. Dordrecht: Kluwer Academic Publishers.
- Maes, D., Gonzalez-Ramirez, L. A., Lopez-Jaramillo, J., Yu, B., De Bondt, H., Zegers, I., Afonina, E., García-Ruiz, J. M. & Gulnik, S. (2004). *Acta Cryst.* **D60**, 463–471.
- Miele, A. E., Federici, L., Sciarra, G., Draghi, F., Brunori, M. & Vallone, B. (2003). *Acta Cryst.* **D59**, 982–988.
- Nedovic, V. & Willaert, R. (2004). Editors. *Fundamentals of Cell Immobilization Biotechnology*. Dordrecht: Kluwer Academic Publishers.
- Nedovic, V. & Willaert, R. (2005). Editors. *Applications of Cell Immobilization Biotechnology*. Dordrecht: Kluwer Academic Publishers.
- Otálora, F. & García-Ruiz, J. M. (1997). *J. Cryst. Growth*, **182**, 141–154.
- Otálora, F., García-Ruiz, J. M., Carotenuto, L., Castagnolo, D., Novella, M. L. & Chernov, A. A. (2002). *Acta Cryst.* **D58**, 1681–1689.
- Robert, M. C., García-Ruiz, J. M., Vidal, O. & Otálora, F. (1999). *Crystallization of Nucleic Acids and Proteins: a Practical Approach*, edited by A. Ducruix & R. Giegé, pp. 149–175. Oxford: IRL Press.
- Robert, M. C. & Lefaucheux, F. (1988). *J. Cryst. Growth*, **90**, 358–367.
- Sauter, C., Lorber, B. & Giegé, R. (2002). *Proteins*, **48**, 146–150.
- Skinner, R., Abrahams, J. P., Whisstock, J. C., Lesk, A. M., Carrell, R. W. & Wardell, M. R. (1997). *J. Mol. Biol.* **266**, 601–609.
- Smith, G. D., Pangborn, W. A. & Blessing, R. H. (2003). *Acta Cryst.* **D59**, 474–482.
- Snell, E. H. & Helliwell, J. R. (2005). *Rep. Prog. Phys.* **68**, 799–853.
- Strong, R. K., Stoddard, B. L., Arrott, A. & Farber, G. K. (1992). *J. Cryst. Growth*, **119**, 200–214.
- Symersky, J., Devedjiev, Y., Moore, K., Brouillette, C. & DeLucas, L. (2002). *Acta Cryst.* **D58**, 1138–1146.
- Thiessen, K. J. (1994). *Acta Cryst.* **D50**, 491–495.
- Tyarkska, E., Lebiada, L., Marchut, E., Steczko, J. & Stec, B. (1990). *J. Protein Chem.* **9**, 83–86.
- Vahedi-Faridi, A., Porta, J. & Borgstahl, G. E. O. (2003). *Acta Cryst.* **D59**, 385–388.
- Vekilov, P. G., Monaco, L. A. & Rosenberger, F. (1995). *J. Cryst. Growth*, **156**, 267–278.
- Vekilov, P. G. & Rosenberger, F. (1996). *J. Cryst. Growth*, **158**, 540–551.

- Vergara, A., Lorber, B., Zagari, A. & Giegé, R. (2003). *Acta Cryst.* **D59**, 2–15.
- Vidal, O., Robert, M. C., Arnoux, B. & Capelle, B. (1999). *J. Cryst. Growth*, **196**, 559–571.
- Vidal, O., Robert, M. C. & Boué, F. (1998a). *J. Cryst. Growth*, **192**, 257–270.
- Vidal, O., Robert, M. C. & Boué, F. (1998b). *J. Cryst. Growth*, **192**, 271–281.
- Villadsen, J. & Michelsen, M. (1978). *Solution of Differential Equations Models by Polynomial Approximation*. Englewood Cliffs, NJ, USA: Prentice-Hall.
- Wardell, M. R., Skinner, R., Carter, D. C., Twigg, P. D. & Abrahams, J.-P. (1997). *Acta Cryst.* **D53**, 622–625.
- Willaert, R. G. & Baron, G. (1996). *Rev. Chem. Eng.* **12**, 2–205.
- Zhu, D.-W., Lorber, B., Sauter, C., Ng, J. D., Le Grimellec, C. & Giegé, R. (2001). *Acta Cryst.* **D57**, 552–558.